



HAL
open science

The Structure and Torsional Dynamics of Two Methyl Groups in 2-Acetyl-5-methylfuran as Observed by Microwave Spectroscopy

Vinh Van, Wolfgang Stahl, Ha Vinh Lam Nguyen

► **To cite this version:**

Vinh Van, Wolfgang Stahl, Ha Vinh Lam Nguyen. The Structure and Torsional Dynamics of Two Methyl Groups in 2-Acetyl-5-methylfuran as Observed by Microwave Spectroscopy. *ChemPhysChem*, 2016, 17 (20), pp.3223-3228. 10.1002/cphc.201600757 . hal-03183106

HAL Id: hal-03183106

<https://hal.science/hal-03183106v1>

Submitted on 26 Mar 2021

HAL is a multi-disciplinary open access archive for the deposit and dissemination of scientific research documents, whether they are published or not. The documents may come from teaching and research institutions in France or abroad, or from public or private research centers.

L'archive ouverte pluridisciplinaire **HAL**, est destinée au dépôt et à la diffusion de documents scientifiques de niveau recherche, publiés ou non, émanant des établissements d'enseignement et de recherche français ou étrangers, des laboratoires publics ou privés.

The structure and torsional dynamics of two methyl groups in 2-acetyl-5-methylfuran as observed by microwave spectroscopy

Vinh Van^[b], Wolfgang Stahl^[b], and Ha Vinh Lam Nguyen^{*[a]}

Abstract The molecular beam Fourier transform microwave spectra of 2-acetyl-5-methylfuran were recorded in the frequency range 2–26.5 GHz. Quantum chemical calculations calculated two conformers with a *trans* and a *cis* configuration of the acetyl group, both of which were assigned in the experimental spectrum. All rotational transitions split into quintets due to the internal rotations of two non-equivalent methyl groups. Using the program *XIAM*, the experimental spectra can be simulated with standard deviations within the measurement accuracy, yielding well-determined rotational and internal rotation parameters, inter alia the V_3 potentials. While the V_3 barrier height of the ring methyl rotor does not change for both conformers, that of the acetyl methyl rotor differs by about 100 cm^{-1} . The predicted values from quantum chemistry are only in the correct order of magnitude.

1. Introduction

Volatile heterocyclic substances are responsible for the aroma during food cooking. For example, the Maillard reaction is known to create desirable aromas in browned food under heating. To understand and explain the smell in more details, it is important to answer the questions how molecular shapes fit together or how strong and how directional hydrogen bonds are. For this purpose, gas phase structures and information on molecular internal dynamics of the Maillard reaction products are needed, since the sense of smell starts from gas phase molecules. Among those products, 2-acetyl-5-methylfuran (AMF) arises from reactions between amino acids and reducing sugars, and produces aroma in cooked food [1]. It was also identified as natural flavor in Chinese liquors [2], smoked salmon [3], as well as roasted coffee beans [4].

Quantum chemically, the relatively small empirical formula of $\text{C}_7\text{H}_8\text{O}_2$ and the known planarity of the furan frame and the acetyl group suggest that structure optimizations are within the capabilities of our computational resources. Since the traditional method by isotopic substitutions is not always possible, the support of quantum chemistry becomes a helpful tool, whereby *ab initio* structures can be taken as references for a comparison of the experimental and calculated molecular parameters.

Spectroscopically, AMF is a derivative of furan with an acetyl substitution on the second ring position and a methyl substitution on the fifth position. When starting this work, we

expected that splittings arising from the internal rotations of both methyl groups can be resolved. The barrier heights of such large amplitude motions (LAM) are mainly determined by steric and electronic effects. While the steric influence is rather local, the electronic contribution can arise from quite distant sources in the molecule, especially when conjugated double bonds and/or aromatic systems are involved. Predicting torsional barriers is challenging because chemical intuition often fails and quantum chemical calculations are still rather inaccurate [5,6]. On the other hand, microwave spectroscopy yields highly accurate torsional barriers. Moreover, two different AMF conformers exist, where at least the acetyl methyl group is exposed to different steric environments, while the ring methyl group is almost unaffected.

2. Quantum Chemical Calculations

From the structural point of view, AMF is rather rigid because the conjugated double bonds in the five-membered ring force the furan frame to be planar. Therefore, the conformational landscape is solely determined by a rotation about the $\text{C}_4\text{-C}_{12}$ bond (for atom numbering see Figure 1). By varying the dihedral angle $\varphi_1 = \angle(\text{O}_{11}, \text{C}_4, \text{C}_{12}, \text{O}_{13})$ in a grid of 2° while all other geometry parameters were optimized at the MP2/6-311++G(d,p) level of theory using the *GAUSSIAN 09* package [7], we obtained a potential energy curve with two minima. The calculated energies were parameterized using a Fourier expansion with the corresponding coefficients given in Table S-1 in the Supporting Information. Using these Fourier coefficients, the potential energy curve was drawn as depicted in Figure 2. Geometries at the minima were fully re-optimized using the HF, B3LYP, M06-2X, MP2, and CCSD methods in combination with various Pople and Dunning basis sets [8,9] to compare the rotational constants and check for convergence. The predicted rotational constants are collected in Table S-2. If not otherwise stated, all values given from now on will refer to those calculated at the MP2/6-311++G(d,p) level of theory. Figure 1 illustrate the fully optimized conformers; their Cartesian coordinates are given in Table S-3. The conformer at $\varphi_1 = 180^\circ$, called the *trans* conformer henceforth, is with zero-point energy correction 4.19 kJ mol^{-1} lower in energy than the so-called *cis* conformer ($\varphi_1 = 0^\circ$).

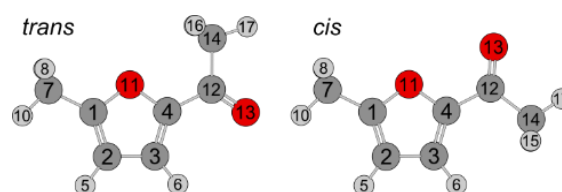


Figure 1. Two conformers of AMF optimized at the MP2/6-311++G(d,p) level of theory.

- [a] Dr. H. V. L. Nguyen
Laboratoire Interuniversitaire des Systèmes Atmosphériques (LISA)
CNRS UMR 7583, Université Paris-Est Créteil, Université Paris
Diderot
61 avenue du Général de Gaulle, F-94010 Créteil cedex, France
E-mail: lam.nguyen@lisa.u-pec.fr
- [b] Vinh Van M. Sc., Prof. Dr. Wolfgang Stahl
Institute of Physical Chemistry
RWTH Aachen University
Landoltweg 2, D-52074 Aachen, Germany

Supporting information for this article is given via a link at the end of the document.

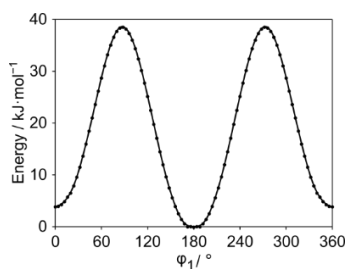


Figure 2. The potential energy curve obtained by varying the dihedral angle $\phi_1 = \angle(\text{O}_{11}, \text{C}_4, \text{C}_{12}, \text{O}_{13})$ in a grid of 2° and optimized at the MP2/6-311++G(d,p) level of theory. Relative energies are given with respect to the lowest energy configuration with its absolute energy $E = -420.930421$ Hartree. The *trans* conformer is located at $\phi_1 = 180^\circ$, the *cis* conformer at 0° .

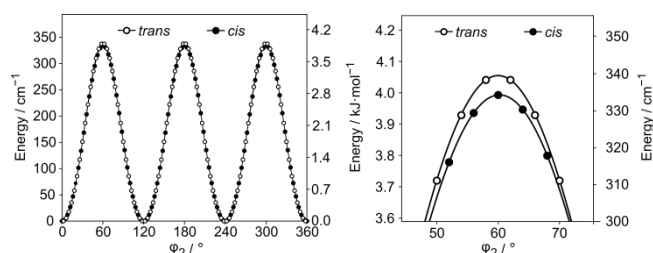


Figure 3. The potential energy curves of the *trans* and the *cis* conformer of AMF obtained by rotating the ring methyl group about the $\text{C}_1\text{--C}_7$ bond. The dihedral angle $\phi_2 = \angle(\text{C}_2, \text{C}_1, \text{C}_7, \text{H}_8)$ was varied in a grid of 2° , while all other molecular parameters were optimized at the MP2/6-311++G(d,p) level. Relative energies with respect to the lowest energy conformations with the absolute energies $E = -420.930421$ and -420.928812 Hartree for the *trans* and the *cis* conformer, respectively, are used. The barrier heights are 340 cm^{-1} for the *trans* and 334 cm^{-1} for the *cis* conformer.

In spite of its relatively simple structure, the internal dynamic of AMF is challenging because of the LAMs of two inequivalent methyl groups, which cause all rotational transitions to split into quintets [10]. The barrier heights of the ring methyl and the acetyl methyl group were calculated by varying the dihedral angles $\phi_2 = \angle(\text{C}_2, \text{C}_1, \text{C}_7, \text{H}_8)$ and $\phi_3 = \angle(\text{O}_{13}, \text{C}_{12}, \text{C}_{14}, \text{H}_{15})$, respectively, in a grid of 2° . A rotation of 120° was sufficient due to the three-fold symmetry of the methyl groups. The potential energy curves of the ring methyl group are shown in Figure 3; the corresponding coefficients in Table S-1 in the Supporting Information. For the *trans* conformer, we found V_3 potentials of 340 cm^{-1} for the ring methyl group and 241 cm^{-1} for the acetyl methyl group with no significant V_6 contributions. The respective values for the *cis* conformer are 334 cm^{-1} and 207 cm^{-1} .

The potential energy curves for a rotation of the acetyl methyl groups are depicted in Figure 4. Here, we expected V_6 contributions for the *trans* conformer due to a more symmetrical environment of the acetyl methyl rotor in relation to both oxygen atoms. Unfortunately, an unusual discontinuity occurred in the minimum regions of the potential curves of this conformer during the rotation of the acetyl methyl group. Therefore, the data set cannot be fitted well. By comparing the two geometries at the discontinued place, we found that (i) only the methyl group was twisted, while all other dihedral angles remain the same, and (ii) one hydrogen atom approaches the eclipse position of the

oxygen atom at this place (see Figure S-1 in the Supporting Information). The barrier height of 241 cm^{-1} obtained from $E(60^\circ) - E(120^\circ)$ is essentially the same as the energy difference between the optimized minimum and the transition state.

As an alternative, geometry optimizations to a first order transition state of the methyl groups were performed at various levels of theory using the Bery algorithm to calculate the barriers to internal rotations [11]. The V_3 potentials predicted at different levels of theory and the angles between the internal rotor axes and the principal axes are summarized in Table S-2.

Finally, a two-dimensional potential energy surface (2D-PES) depending on ϕ_2 and ϕ_3 were performed by varying these two dihedral angles in a grid of 10° to study the coupling between the two LAMs of the methyl groups. Due to symmetry, only data points in the range from ϕ_2 and $\phi_3 = 0^\circ$ to 120° are needed. The potential energies were parameterized with a 2D Fourier expansion based on terms representing the correct symmetry of the angles ϕ_2 and ϕ_3 . The corresponding coefficients are given in Table S-1 in the Supporting Information. The PES illustrated in Figure 5 exhibits almost no potential coupling terms between ϕ_2 and ϕ_3 for both conformers.

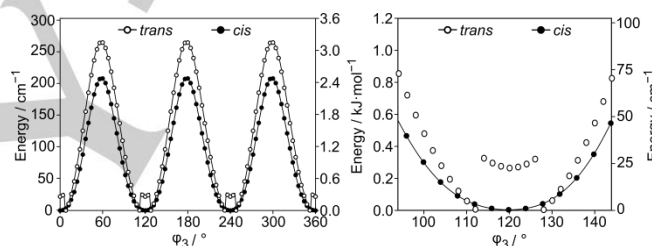


Figure 4. The potential energy curves of the *trans* and the *cis* conformer of AMF obtained by rotating the acetyl methyl group about the $\text{C}_{12}\text{--C}_{14}$ bond. The dihedral angle $\phi_3 = \angle(\text{O}_{13}, \text{C}_{12}, \text{C}_{14}, \text{H}_{15})$ was varied in a grid of 2° , while all other molecular parameters were optimized at the MP2/6-311++G(d,p) level. Relative energies with respect to the lowest energy conformations with the absolute energies $E = -420.930421$ and -420.928812 Hartree for the *trans* and the *cis* conformer, respectively, are given. The barrier height is 207 cm^{-1} for the *cis* conformer. For the *trans* conformer, an unusual discontinuity occurred in the minimum regions, as can be recognized in the enlarged scale (right hand side figure).

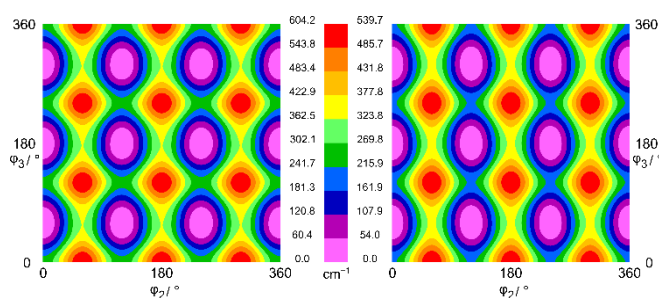


Figure 5. The potential energy surface depending on the dihedral angles $\phi_2 = \angle(\text{C}_2, \text{C}_1, \text{C}_7, \text{H}_8)$ and $\phi_3 = \angle(\text{O}_{13}, \text{C}_{12}, \text{C}_{14}, \text{H}_{15})$ of the *trans* (left hand side) and the *cis* conformer (right hand side) of AMF calculated at the MP2/6-311++G(d,p) level of theory. ϕ_2 and ϕ_3 were varied in a grid of 10° , while all other parameters were optimized. The relative energy maxima are 604.2 cm^{-1} (7.2 kJ mol^{-1}) and 539.7 cm^{-1} (6.5 kJ mol^{-1}) for the *trans* and the *cis* conformer, respectively.

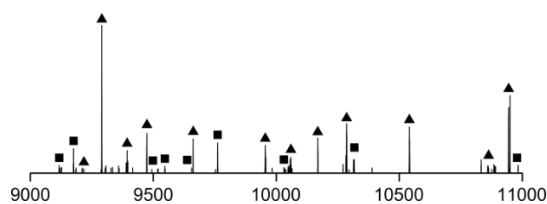


Figure 6. A portion of the broadband scan from 9000 to 11000 MHz of AMF showing that (i) transitions of the *trans* conformer (▲) are much more intense than those of the *cis* conformer (■), and (ii) only a few unassigned lines are present in the spectrum.

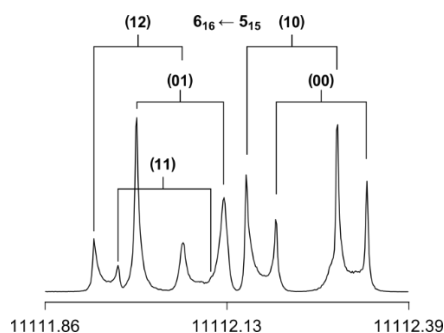


Figure 7. A typical spectrum of the $6_{16} \leftarrow 5_{15}$ transition of the *trans* conformer of AMF with its (00), (10), (01), (11), and (12) torsional species. The frequency is in MHz; the line width is approximately 13 – 25 kHz (FWHM), corresponding to a measurement accuracy of 2 kHz. The splittings indicated by brackets are due to the Doppler effect. For this spectrum 2000 decays were co-added.

3. Microwave spectroscopy

We started the assignment with the spectrum of the more stable *trans* conformer, which has dipole moment components of 4.14 D, 1.67 D, and 0.00 D in *a*-, *b*-, and *c*-direction, respectively. Only *a*- and *b*-type transitions are expected in the spectrum, and *a*-type lines should be more intense. The selection rules for *a*-type lines are $K_a K_c$: $ee \leftrightarrow eo$ and $oo \leftrightarrow oe$ and for *b*-type lines $K_a K_c$: $ee \leftrightarrow oo$ and $oe \leftrightarrow eo$ ($e = \text{even}$, $o = \text{odd}$) [12]. At the beginning, we neglected the internal rotation effects and considered AMF as a rigid rotor. A prediction carried out with the program XIAM [13] indicated a relatively dense spectrum in the frequency range from 9.0 to 13.0 GHz. A broadband scan was recorded in this region, where overlapping spectra in a step size of 0.25 MHz were automatically recorded. Figure 6 shows a portion of the scan. All lines indicated in the scan were re-measured at higher resolution. A typical high resolution spectrum is shown in Figure 7.

The $J = 5 \leftarrow 4$ *a*-type transitions with $K_a = 0, 1$ and the *b*-type $6_{06} \leftarrow 5_{15}$ and $7_{07} \leftarrow 6_{16}$ as well as $4_{14} \leftarrow 3_{03}$, $5_{15} \leftarrow 4_{04}$, and $6_{16} \leftarrow 5_{05}$ transitions were readily assigned. Each transition splits into five torsional component $(\sigma_1 \sigma_2) = (00), (01), (10), (11), \text{ and } (12)$ because of the LAMs of two methyl groups [10]. The notations σ_1 and σ_2 refer to the ring methyl rotor and the acetyl methyl rotor, respectively. The assignment of these lines enabled us to predict and find further (00) transitions.

In the next step, we took the methyl internal rotations into consideration and predicted a two-top fit using the rotational

Table 1. Molecular parameters of the *trans* and the *cis* conformer of AMF as obtained by the program XIAM. Top 1 refers to the ring methyl group, top 2 to the acetyl methyl group.

Par. ^[a]	Unit	<i>trans</i>	MP2 ^[b]	<i>cis</i>	MP2 ^[b]
<i>A</i>	GHz	3.699650628(73)	3.638	3.9138572(37)	3.843
<i>B</i>	GHz	1.125952913(72)	1.120	1.09556167(24)	1.089
<i>C</i>	GHz	0.872880211(49)	0.866	0.86550261(12)	0.858
<i>D_J</i>	kHz	0.03511(28)	0.03449	0.0294(20)	0.03042
<i>D_{JK}</i>	kHz	-0.0392(29)	-0.04428	-0.050(17)	-0.03050
<i>D_K</i>	kHz	1.10(17)	0.7370	0.783(71)	0.7145
<i>d₁</i>	kHz	-0.01066(20)	-0.01036	-0.0066(14)	-0.008137
<i>d₂</i>	kHz	-0.00124(16)	-0.0009489	0.00 ^[c]	-0.0002910
<i>V_{3,1}</i>	cm ⁻¹	369.78(25)	340.	356.47(39)	334.
<i>F_{0,1}</i>	GHz	159.40(11)	159.3	159.16(16)	159.2
$\angle(i_1, a)$	°	143.601(34)	143.11	146.523(69)	146.36
$\angle(i_1, b)$	°	126.399(34)	126.89	123.477(69)	123.64
$\angle(i_1, c)^{[d]}$	°	90.0	90.00	90.0	90.00
<i>V_{3,2}</i>	cm ⁻¹	307.78(59)	241	212.71(30)	207
<i>F_{0,2}</i>	GHz	160.51(39)	158.0	159.87(24)	158.1
$\angle(i_2, a)$	°	75.154(31)	78.59	-41.012(15)	-44.48
$\angle(i_2, b)$	°	165.154(31)	168.59	48.988(15)	45.52
$\angle(i_2, c)^{[d]}$	°	90.0	89.99	90.0	90.00
<i>D_{pi2J,2}</i>	kHz	40.36(47)		18.78(34)	
<i>D_{pi2K,2}</i>	kHz	-206.5(61)		-343(24)	
$\sigma^{[e]}$	kHz	2.4		2.6	
<i>N^[f]</i>		280		105	

[a] All parameters are given with one standard uncertainty in parentheses. Watson's S reduction and I' representation was used. [b] Vibrational ground state B_0 rotational constants and centrifugal distortion constants obtained by anharmonic frequency calculation at the MP2/6-311++G(d,p) level of theory. [c] Not fitted, set to zero. [d] Fixed due to symmetry. [e] Standard deviation of the fit. [f] Number of lines.

constants from the rigid rotor fit. The angles δ between the internal rotor axes and the principal *a* axis as well as the V_3 potentials were calculated by *ab initio*. The LAM splittings are relatively small (up to 20 MHz), which simplified the assignment. Some rotational transitions exhibited very small splittings down to a few kHz. The assignment of those transitions was quite challenging because different torsional species could not be easily distinguished. Finally, 280 torsional transitions with $J \leq 10$ were assigned and fitted to a standard deviation of 2.4 kHz using the program XIAM. The results of the fits are given in Table 1.

After the *trans* conformer was assigned, many lines with low intensities remained in the scan which presumably belong to the *cis* conformer with the calculated dipole moment components of 2.26 D, 4.04 D, and 0.00 D in *a*-, *b*-, and *c*-direction, respectively. Also in this case, the spectrum contains only *a*- and *b*-type transitions and *b*-type lines should be more intense. Surprisingly, the $J = 5 \leftarrow 4$ and $6 \leftarrow 5$ *a*-type transitions could be assigned first and they were more intense than most of the *b*-type lines. For the *cis* conformer, 105 torsional transitions up to $J = 8$ were measured and fitted to a standard deviation of 2.6 kHz (see Table 1). The frequency lists of both, the *trans* and the *cis* conformer, are available in Table S-4 in the Supporting Information.

4. Results and Discussion

The three linear combinations of the rotational constants $B_J = \frac{1}{2}(B + C)$, $B_K = A - \frac{1}{2}(B + C)$, $B_- = \frac{1}{2}(B - C)$ and the centrifugal

distortion constants D_J , D_{JK} , D_K , d_1 , d_2 were determined with very high accuracy for both conformers. The V_3 potentials, the angles δ between the internal rotor axes and the principal a axis, the internal rotation constant, and two higher order parameters D_{p2J} and D_{p2K} were also fitted.

The experimentally deduced rotational constants are compared with those from quantum chemical calculations. Best agreements can be found with the DFT method using the functionals M06-2X and B3LYP for the *trans* and the *cis* conformer, respectively, as shown in Table S-2 in the Supporting Information. All levels of theory yield quite reasonable B and C rotational constants, while the A rotational constant has larger deviations. We note that all predicted rotational constants reported in Table S-2 refer to the equilibrium r_e structure, while the experimentally deduced rotational constants to the vibrational ground state r_0 structure. Theoretical rotational constants of the r_0 structure can be obtained by anharmonic frequency calculation (given in Table 1). Surprisingly, they show larger deviations to the experimental values compared to those of the r_e structure. This is probably due to error compensations. For more details, the vibration-rotation constants for each vibrational mode are given in Table S-5 in the Supporting Information.

Because of the strong correlation between V_3 and F_0 in the fit shown in Table 1, we carried out a fit with F_0 fixed to the *ab initio* values (given in Table S-6). The V_3 terms, which depend on the assumed values of F_0 , as well as the higher order parameters D_{p2J} and D_{p2K} change slightly. The V_6 term cannot be fitted independently, because only transitions in the torsional ground state are available, and we set it to zero. Since the *ab initio* results predict no significant V_6 contributions (see section 2), we expect that the experimental values of the V_3 terms are sufficiently accurate.

The calculated centrifugal distortion constants obtained by anharmonic frequency calculations with the MP2 and B3LYP methods and the basis set 6-311++G(d,p) are in good agreement with the experimental values except for the parameter D_K of the *trans* conformer (see Table 1). Since the planar five-membered ring frame of AMF is quite rigid, all centrifugal distortion constants are small. We recognized a relatively strong correlation between the parameters B_K and D_K in the fit of the *trans* conformer, if F_0 is fixed to its *ab initio* values (see Table S-7 in the Supporting Information). This correlation decreases slightly if F_0 is fitted (as in the fit shown in Table 1; for the correlation matrices see also Table S-7), and the D_K value is closer to the predicted value.

The barrier heights of the ring methyl top are $369.78(25)$ cm^{-1} and $356.47(39)$ cm^{-1} for the *trans* and the *cis* conformer, respectively, which are very similar. Obviously, the orientation of the acetyl group does not significantly affect the torsional barrier of the ring methyl group. On the other hand, the barrier heights are clearly lower than that found in 2-methylfuran (416.2 cm^{-1}) [14], showing that the presence of the acetyl methyl group with its negative mesomeric effect and the possibility for an extended π -conjugation might decrease the barrier of the ring methyl group.

The barrier to internal rotation of the acetyl methyl top is quite different in two conformers. We found a value of $307.78(59)$ cm^{-1} for the *trans* and $212.71(30)$ cm^{-1} for the *cis*

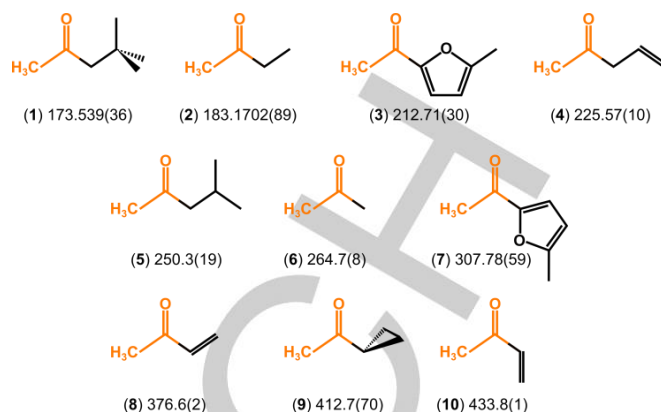


Figure 8. Torsional barriers of the acetyl methyl groups in ketones (in cm^{-1}). (1) Methyl neopentyl ketone [13], (2) methyl ethyl ketone [14], (3) *cis* AMF (this work), (4) allyl acetone [15], (5) methyl isobutyl ketone [16], (6) acetone [17], (7) *trans* AMF (this work), (8) *syn*-periplanar-methyl vinyl ketone [18], (9) cyclopropyl methyl ketone [19], (10) *anti*-periplanar-methyl vinyl ketone [18].

conformer. From many previous investigations, it is known that the torsional barrier of the acetyl methyl group in ketones depends strongly on the substitution at the other side of the carbonyl group, as can be seen in Figure 8 [15-21]. This behavior in ketones, where the substituent on the other side of the carbonyl group causes the acetyl methyl barrier to vary over a wide range without any apparent trends, is in strong contrast to the acetates, which can be divided in classes with predictable barrier heights [22]. For example in α,β -saturated alkyl acetates, the barrier to internal rotation is approximately 100 cm^{-1} and remains largely invariant [23,24]. This value cannot be easily predicted when electronic effect exists, e.g. by the presence of double bonds or lone electron pairs, which can contribute in a conjugated system. In unsaturated acetates like vinyl acetate [25] and isopropenyl acetate [26], π -electron conjugation, extending from the vinyl double bond to the ester group, is possible. The barriers are significantly different and also differ from those found for saturated acetates. In some acetamides such as N-ethylacetamide [27] or N,N-diethylacetamide [5], it turns out that the barriers of the acetyl methyl group are strongly affected by the electronic effect from the lone electron pair and the substituents attached to the nitrogen. We note that though AMF is different from other ketones because of the aromatic ring, the barrier height in its both conformers is not unusually larger or smaller. Similar to the case of N,N-diethylacetamide [5] and methyl vinyl ketone [20], the barrier height of the acetyl methyl rotor depends strongly on the orientation of the substituent on the other side of the carbonyl group. Further conclusions cannot be drawn since too few ketone examples are available at the moment.

The calculated torsional barriers of the ring methyl group at different levels of theory are $297 - 501$ cm^{-1} and $283 - 477$ cm^{-1} for *trans* and the *cis* conformer, respectively, which are in the same order of magnitude of the experimental V_3 potentials. For the acetyl methyl top, we found $162 - 349$ cm^{-1} for the *trans* and $71 - 311$ cm^{-1} for the *cis* conformer. The best agreement

between the calculated and experimental barriers were found for both conformers and both methyl groups at the M06-2X/6-311++G(3df,2pd) level of theory (see Table S-2).

The inertial defects $\Delta_c = (I_c - I_a - I_b) = -6.469$ and -6.580 $\text{u}\text{\AA}^2$ of the *trans* and *cis* conformers, respectively, confirm that the heavy atom skeleton is planar with two pairs of hydrogen atoms out of plane. These values are almost the same as that found in other planar molecules containing two methyl groups with comparable barrier heights, e.g. methyl acetate ($\Delta_c = -6.315$ $\text{u}\text{\AA}^2$) [28] and the *syn* and *anti* conformers of 3,4-dimethylbenzaldehyde ($\Delta_c = -6.452$ and -6.469 $\text{u}\text{\AA}^2$, respectively) [29].

After the assignment of the two conformers, only very few weak lines remained in the broadband scan. We thus concluded that water complexes or dimers were not present under our measurement conditions.

5. Conclusion

Two conformers of 2-acetyl-5-methylfuran exhibiting the internal rotations of two non-equivalent methyl groups were successfully assigned under molecular beam conditions using a combination of Fourier-transform microwave spectroscopy and quantum chemistry. The above mentioned intramolecular dynamics causes splittings of all rotational transitions into five different torsional species. The torsional barriers of the ring methyl top are similar in both conformers; those of the acetyl methyl group are on the other hand quite different, which is probably because of the electronic rather than the steric effect. Quantum chemical calculations yielded reasonable structural parameters, but the predicted barrier heights are not yet sufficiently accurate.

Experimental Section

The rotational spectra were measured with a molecular beam Fourier transform microwave spectrometer operating in the frequency range from 2 to 26.5 GHz [30]. AMF was purchased from TCI Deutschland GmbH, Eschborn, Germany with a stated purity of over 97 % and used without further purification. The sample was placed on a 5 cm piece of a pipe cleaner inside a stainless steel tube mounted upstream the nozzle. Helium was flown over the sample at a pressure of approximately 200 kPa, the helium-substance mixture was expanded into the cavity.

Acknowledgements

V. V. thanks the Fonds der Chemischen Industrie (FCI) for a Ph.D. fellowship. Simulations were performed with computing resources granted by JARA-HPC from the RWTH Aachen University under the project jara0124.

Keywords: internal rotation • large amplitude motion • rotational spectroscopy • quantum chemical calculation

- [1] L. J. Farmer, D. S. Mottram, F. B. Whitfield, *J. Sci. Food Agric.* **1989**, *49*, 347-368.
[2] W. Fan, M. C. Quian, *J. Agric. Food Chem.* **2006**, *54*, 2695-2704.

- [3] V. Varlet, C. Knockaert, C. Prost, T. Serot, *J. Agric. Food Chem.* **2006**, *54*, 3391-3401.
[4] D. Ryan, R. Shellie, P. Tranchida, A. Casilli, L. Mondello, P. Marriott, *J. Chromatogr. A* **2004**, *1054*, 57-65.
[5] R. Kannengießer, S. Klahm, H. V. L. Nguyen, A. Lüchow, W. Stahl, *J. Chem. Phys.* **2014**, *141*, 204308.
[6] V. Van, W. Stahl, H. V. L. Nguyen, *Phys. Chem. Chem. Phys.* **2015**, *17*, 32111-32114.
[7] M. J. Frisch, G. W. Trucks, H. B. Schlegel, G. E. Scuseria, M. A. Robb, J. R. Cheeseman, G. Scalmani, V. Barone, B. Mennucci, G. A. Petersson, H. Nakatsuji, M. Caricato, X. Li, H. P. Hratchian, A. F. Izmaylov, J. Bloino, G. Zheng, J. L. Sonnenberg, M. Hada, M. Ehara, K. Toyota, R. Fukuda, J. Hasegawa, M. Ishida, T. Nakajima, Y. Honda, O. Kitao, H. Nakai, T. Vreven, J. A., Jr. Montgomery, J. E. Peralta, F. Ogliaro, M. Bearpark, J. J. Heyd, E. Brothers, K. N. Kudin, V. N. Staroverov, R. Kobayashi, J. Normand, K. Raghavachari, A. Rendell, J. C. Burant, S. S. Iyengar, J. Tomasi, M. Cossi, N. Rega, J. M. Millam, M. Klene, J. E. Knox, J. B. Cross, V. Bakken, C. Adamo, J. Jaramillo, R. Gomperts, R. E. Stratmann, O. Yazyev, A. J. Austin, R. Cammi, C. Pomelli, J. W. Ochterski, R. L. Martin, K. Morokuma, V. G. Zakrzewski, G. A. Voth, P. Salvador, J. J. Dannenberg, S. Dapprich, A. D. Daniels, O. Farkas, J. B. Foresman, J. V. Ortiz, J. Cioslowski, D. J. Fox, Gaussian 09, Revision A.02, Gaussian, Inc., Wallingford CT, **2009**.
[8] R. Ditchfield, W. J. Hehre, J. A. Pople, *J. Chem. Phys.* **1971**, *54*, 724-728.
[9] T. H. Dunning Jr., *J. Chem. Phys.* **1989**, *90*, 1007-1023.
[10] H. Dreizler, *Z. Naturforsch.* **1961**, *16a*, 1354-1367.
[11] H. B. Schlegel, *J. Comput. Chem.* **1982**, *3*, 214-218.
[12] W. Gordy, R. L. Cook, *Microwave Molecular Spectra*, John Wiley & Sons, New York **1984**, 3rd edition.
[13] H. Hartwig, H. Dreizler, *Z. Naturforsch. A* **1996**, *51*, 923-932.
[14] W. G. Norris, L. C. Krisher, *J. Chem. Phys.* **1969**, *51*, 403-406.
[15] Y. Zhao, J. Jin, W. Stahl, I. Kleiner, *J. Mol. Spectrosc.* **2012**, *281*, 4-8.
[16] H. V. L. Nguyen, V. Van, W. Stahl, I. Kleiner, *J. Chem. Phys.* **2014**, *140*, 214303.
[17] L. Tulimat, H. Mouhib, W. Stahl, I. Kleiner, *J. Mol. Spectrosc.* **2015**, *312*, 46-50.
[18] Y. Zhao, W. Stahl, H. V. L. Nguyen, *Chem. Phys. Lett.* **2012**, *545*, 9-13.
[19] R. Peter, H. Dreizler, *Z. Naturforsch.* **1965**, *20a*, 301-312.
[20] D. S. Wilcox, A. J. Shirar, O. L. Williams, B. C. Dian, *Chem. Phys. Lett.* **2011**, *508*, 10-16.
[21] P. L. Lee, R. H. Schwendeman, *J. Mol. Spectrosc.* **1972**, *41*, 84-94.
[22] A. Jabri, V. Van, H. V. L. Nguyen, W. Stahl, I. Kleiner, *ChemPhysChem* **2016**, DOI: 10.1002/cphc.201600265.
[23] D. Jelisavac, D. C. Cortés-Gómez, H. V. L. Nguyen, L. W. Sutikdja, W. Stahl, I. Kleiner, *J. Mol. Spectrosc.* **2009**, *257*, 111-115.
[24] L. W. Sutikdja, W. Stahl, V. Sironneau, H. V. L. Nguyen, I. Kleiner, manuscript accepted in *Chem. Phys. Lett.* **2016**.
[25] H. V. L. Nguyen, A. Jabri, V. Van, W. Stahl, *J. Phys. Chem. A* **2014**, *118*, 12130-12136.
[26] H. V. L. Nguyen, W. Stahl, *J. Mol. Spectrosc.* **2010**, *264*, 120-124.
[27] R. Kannengießer, M. J. Lach, W. Stahl, H. V. L. Nguyen, *ChemPhysChem* **2015**, *9*, 1906-1911.
[28] M. Tudorie, I. Kleiner, J. T. Hougen, S. Melandri, L. W. Sutikdja, W. Stahl, *J. Mol. Spectrosc.* **2011**, *269*, 211-225.
[29] M. Tudorie, I. Kleiner, M. Jahn, J.-U. Grabow, M. Goubet, O. Pirali, *J. Phys. Chem. A* **2013**, *117*, 13636-13647.
[30] J.-U. Grabow, W. Stahl, H. Dreizler, *Rev. Sci. Instrum.* **1996**, *67*, 4072-4084.

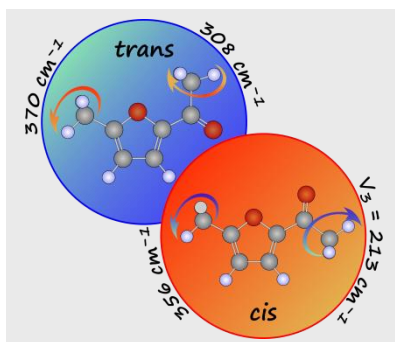
Entry for the Table of Contents (Please choose one layout)

Layout 1:

ARTICLE

Hard to guess - The torsional barriers of methyl groups

Two different conformers of 2-acetyl-5-methylfuran with two non-equivalent methyl groups each were analyzed by microwave spectroscopy. The barriers to internal rotation were accurately determined. Quantum chemistry yields only the correct order of magnitude while chemical intuition fails completely.



Vinh Van, Wolfgang Stahl, Ha Vinh Lam Nguyen*

Page No. – Page No.

The structure and torsional dynamics of two methyl groups in 2-acetyl-5-methylfuran as observed by microwave spectroscopy